Accepted Manuscript

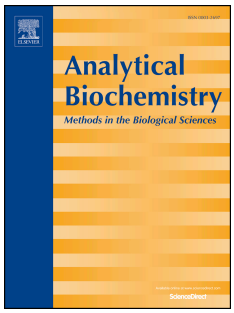

Construction of Quenchbodies to detect and image amyloid β oligomers

Jinhua Dong, Richi Fujita, Tamotsu Zako, Hiroshi Ueda

PII: S0003-2697(18)30420-2

DOI: 10.1016/j.ab.2018.04.016

Reference: YABIO 12996

To appear in: *Analytical Biochemistry*

Received Date: 19 December 2017

Revised Date: 13 April 2018

Accepted Date: 16 April 2018

Please cite this article as: J. Dong, R. Fujita, T. Zako, H. Ueda, Construction of Quenchbodies to detect and image amyloid β oligomers, *Analytical Biochemistry* (2018), doi: 10.1016/j.ab.2018.04.016.

Construction of Quenchbodies to Detect and Image Amyloid β oligomers

Jinhua Dong[1,2], Richi Fujita[3], Tamotsu Zako[4], Hiroshi Ueda[2*]

[1]*Key Laboratory of Biological Medicine in Universities of Shandong Province, School of Bioscience and Technology, Weifang Medical University, 7166 Baotongxi, Weifang, Shandong 261053, P.R. China.*

[2]*Laboratory for Chemistry and Life Science, Institute of Innovative Research, Tokyo Institute of Technology, 4259 Nagatsuta-cho, Midori-ku, Yokohama, Kanagawa 226-8503 Japan*

[3]*Department of Chemistry and Biotechnology, School of Engineering, The University of Tokyo, 7-3-1 Hongo, Bunkyo-ku, Tokyo 113-8656 Japan*

[4]*Department of Chemistry and Biology, Graduate School of Science and Engineering, Ehime University, 2-5, Bunkyo-cho, Matsuyama, Ehime 790-8577 Japan*

[*]Corresponding author: Tel./Fax: +81 45-924-5248. E-mail address: ueda@res.titech.ac.jp

Running title: Quenchbodies to detect Amyloid β oligomers

Abstract

A quenchbody (Q-body) is an antibody-based biosensor that employs fluorescence quenching of the dye(s) attached to the antibody fragment, which are de-quenched upon antigen binding. In this study, we aimed to develop Fab type Q-bodies (UQ-bodies) to aid the diagnosis of Alzheimer's disease (AD). Characteristic senile plaques in AD consist of amyloid-β peptide (Aβ) generated from the amyloid precursor protein. Aβ42, one of the major peptide forms, aggregates fast and manifests higher neurotoxicity. Recent studies showed that Aβ oligomers, such as Aβ-derived diffusible ligand (ADDL), are more toxic than fibrils. Thus, detection of Aβ and its oligomers in body fluid might help detect deterioration caused by the disease. To this end, the Fab fragment of the anti-Aβ antibody h12A11, which binds preferentially to ADDL, was expressed in *Escherichia coli*, and labeled with a fluorescent dye at the N terminus of either the heavy chain, or the heavy and light chains, via Cys-containing tag(s) to prepare UQ-bodies. As a result, the double-labeled UQ-bodies detected ADDL with higher sensitivity than that for the Aβ peptide. In addition, the UQ-body could be used to image aggregated Aβ with a low background, which suggested the potential of UQ-bodies as a fast bioimaging tool.

Key words: Amyloid; homogeneous immunoassay; recombinant antibody; fluorescence; oligomers;

Introduction

Quenchbody (Q-body) immunoassay is a novel biosensing technology that uses the quenching of fluorescence by intrinsic tryptophan (Trp) residues in antibody variable regions when dye(s) are conjugated to an antibody or antibody fragments in appropriate position, and de-quenching while the antibody binds to the antigen. Compared with conventional fluoroimmunoassays, the Q-body assay is simple, and requires no additional reagents to perform the detection [1, 2]. We also found that Q-bodies prepared with antigen binding fragments (Fab) of an antibody (ultra Q-body, UQ-body) generally produce a larger fluorescence increase when bound to the antigen compared with Q-bodies comprising a single chain variable region Fv (scFv) [3]. To date, Q-bodies to detect small chemicals, including illegal drugs [1], pesticides [4], peptides [3], and also larger proteins including cancer-related membrane protein claudin [5], have been developed.

Alzheimer's disease (AD) is a serious disease of the elderly and has been studied for many years. Progressive dementia in AD is associated with selective neuronal degeneration and death [6]. AD is characterized by two pathological features in the brain: Extracellular senile plaques and intracellular neurofibrillary tangles. Senile plaques consist of amyloid-β peptide (Aβ), which is generated from amyloid precursor protein (APP) through sequential proteolytic processing by β-secretase and γ-secretase. Aβ42, one of the major peptide forms, aggregates faster than other peptides, and results in higher neurotoxicity [7]. Historically, Aβ fibrils have been considered to be primarily responsible for neuronal dysfunction and death, because fibrils were detectable in diseased brains and led to neuronal dysfunction, dystrophy, and synaptic loss [8, 9]. Busciglio et al. demonstrated that amyloid fibril formation alters the phosphorylation of tau, which leads to loss of its microtubule binding capacity [10]. Until now, the post mortem identification of amyloid plaques consisting of the Aβ peptide, and

neurofibrillary tangles in the brains of the patients are the most reliable diagnosis of AD. Great efforts are being made to identify reliable biomarkers that are suitable for minimal invasive early diagnosis and prognosis of AD. During the past years, body fluids of AD patients were assayed for their content of total or soluble Aβ40 or Aβ42 using classical methods, such as enzyme-linked immunosorbent assay (ELISA) or non-classical readout [11, 12]. The presence of Aβ aggregates seems to be the most direct disease biomarker for AD and increasing effort is being made to develop methods suitable to detect different Aβ aggregates in body fluids, such as cerebrospinal fluid (CSF) and plasma. Recent studies showed that soluble Aβ oligomers, such as Aβ-derived diffusible ligand (ADDL), are more toxic than fibrils [13, 14]. ADDL binds to neurons and attacks memory-synapses, and has been identified in actual AD brains [15]. In this study, we aimed to develop UQ-bodies to detect the Aβ peptide and its oligomers.

Materials and Methods

Materials

Escherichia coli strain XL10-Gold (Stratagene, La Jolla, CA, USA) was used for general cloning, and strain SHuffle T7 expressing lysY (New England Biolabs, Ipswich, MA, USA) was used for protein expression. Restriction-modification enzymes were purchased from Takara-Bio (Shiga, Japan), Toyobo Biochemicals (Osaka, Japan), Roche Diagnostics (Tokyo, Japan), or New England Biolabs. The gene encoding the humanized variable regions of antibody 12A11 [16] (h12A11, based on the sequences 34 and 35 in Patent WO2006/066089 for V_L and V_H, respectively) was synthesized by Greiner Bio One (Tokyo, Japan). Biotinylated DAE10 peptide (bio-DAE10; NH_2-DAEFRHDSGYSGENRSDQK(biotin)GEGGC-COOH) [16] was synthesized by LifeTein

(Hillsborough, NJ, USA) and oligonucleotides were synthesized by Greiner Bio One. Other chemicals, reagents, and antibodies, unless otherwise indicated, were obtained from Sigma (St. Louis, MO, USA) or Wako Pure Chemicals (Osaka, Japan).

Construction of the plasmid for the expression of the antibody fragments

Previously, we constructed a vector, pUQ1H-KTM219, to express the Fab of anti-osteocalcin antibody KTM219 with an additional cysteine at the N terminus of V_H [3], and pUQ1HGS-HODE and pUQ2GS-HODE for the expression of Fab fragments of an antibody against 13(S)-hydroxy-9E,11E-octadecadienoic acid (unpublished). By deletion of the genes encoding V_H and V_L from the above vectors and the addition of genes encoding antibody h12A11, which binds stronger to Aβ oligomers than monomer, we constructed vector pUQ1H-h12A11 to express the Fab of h12A11 with a Cys-tag (MAQIEVNCSN) on the N terminus of heavy chain, pUQ1HGS-h12A11 to express the Fab with a Cys-tag and a GS linker (GGGSGGTG) on the N terminus of the heavy chain, and pUQ2GS-h12A11 with a Cys-tag and a GS linker on the N-termini of both the heavy and light chains (Figure 1).

Briefly, to construct pUQ1H-h12A11, the V_L gene of h12A11 was amplified by polymerase chain reaction (PCR) using plasmid pIT2-h12A11, which contains the gene for h12A11, as a template and the primers RV_Vkh12A11 and JkHind_h12A11. The sequences of the primers used in this study are shown in Table 1. The PCR products were purified and digested with *Eco*RV/*Hin*dIII. pUQ1H-KTM219 was digested with same enzymes and the longer fragment was purified and ligated with the *Eco*RV/*Hin*dIII-digested V_L gene using Ligation High ver.2 (Toyobo Biochemicals). *E. coli* XL10-Gold cells were transformed with the mixture and cultivated on Luria-Bertani (LB) plates (1.0% tryptone, 0.5% yeast extract, 0.5% NaCl, 1.5% agar) with 100 μg/ml ampicillin at 37 °C overnight. The colonies

containing the target plasmid were screened by colony PCR using primers T7promoter and T7terminator, and positive clones were cultivated to prepare the plasmid. Plasmids containing the V_L gene of h12A11 was further digested with *Age*I/*Xho*I to remove the V_H gene of KTM219 and inserted with the V_H gene of h12A11, amplified with primers Age_VHh12A11 and JHXho_h12A11, and digested with *Age*I/*Xho*I to construct the plasmid pUQ1H-h12A11 (Figure 1A).

Plasmid pUQ1HGS-h12A11, which expresses the Fab with a GS linker (GGGSGGTG) downstream of the Cys-tag (Figure 1B), and pUQ2GS-h12A11 expressing the Fab with Cys-tag and GS linkers on N termini of both V_H and V_L (Figure 1C), were constructed based on a previously constructed vectors pUQ1HGS-HODE and pUQ2GS-HODE. Plasmid pUQ1HGS-h12A11 was constructed using the same protocol as that for pUQ1H-h12A11. To construct pUQ2GS-h12A11, the V_L gene for h12A11 was amplified with primers Spe_Vkh12A11 and JkHind_h12A11 and cloned into the *Spe*I/*Hin*dIII enzyme sites of pUQ2GS-HODE, and then the V_H gene was cloned into the resulting plasmid using the same protocol used to construct pUQ1GS-h12A11. The nucleic acid sequences of the resulting plasmids were analyzed by the Division of Biomaterial Analysis, Technical Department, Tokyo Institute of Technology.

Expression and purification of antibody fragments

E. coli SHuffle T7 express lysY cells were transformed with the plasmids and cultured on LB agar containing 100 μg/ml ampicillin (LBA) at 30 °C overnight. A single colony was picked up and cultivated in liquid LBA medium until the OD_{600} reached 0.5, at which point 0.4 mM isopropylthio-β-galactopyranoside was added to induce protein expression. The culture was continued for 16 h with shaking at 200 rpm at 16 °C. Intracellular soluble

proteins were extracted by sonication and purified using Talon immobilized metal affinity resin, according to the manual provided by manufacturer (Clontech, Takara-Bio).

Preparation of ADDL

ADDL was prepared using the protocol reported by Lambert et al. [15]. In brief, powdered Aβ42 (Peptide Institute, Inc., Ibaraki, Osaka, Japan) was dissolved in anhydrous dimethyl sulfoxide (DMSO) at 5 mM to make a pre-ADDL stock solution. Pre-ADDL was diluted into Ham's medium to a final concentration of 100 μM, and incubated at 4 °C for 24 h to prepare the ADDL solution.

Preparation of Q-bodies

The purified Fab was subjected to a Nanosep Centrifugal-10 k Ultrafiltration Device and equilibrated with phosphate buffer (50 mM sodium phosphate, 100 mM NaCl, 10 mM EDTA, pH 7.0). A volume of immobilized Tris (2-carboxyethyl)phosphine Hydrochloride (TCEP-HCl) Disulfide Reducing Gel slurry (Pierce, Thermo Fisher Scientific, Rockford, IL) equal to the volume of the purified protein was added to a microtube and centrifuged at 50 × *g* for 1 min. After removing the supernatant, the purified protein was added and incubated for 1 h at room temperature on a rotating wheel. After centrifugation for 1 min, the supernatant was recovered and its concentration was determined using the Bradford assay (Bio-Rad) with bovine serum albumin (BSA) as the standard.

The reduced protein was labeled with TAMRA-C5-maleimide (TMRC5), TAMRA-C6-maleimide (TMRC6), or ATTO520-maleimide in the dark for 2 h at 25 °C. The molar ratio of protein to dye was 1:10. The product was subsequently incubated with 20 μl of Anti DYKDDDDK tag Antibody Beads (Wako). After incubation at room temperature for 2

h, the beads were washed three times with wash buffer (20 mM phosphate, 0.5 M NaCl, 0.1% polyoxyethylene(23) laurylether, pH 7.4). The bound proteins were subsequently eluted with two 200-µl volumes of wash buffer containing 150 µg/ml of the DYKDDDDK peptide (Wako).

To confirm the amount and purity of the UQ-bodies, 10 µl of each sample were separated by sodium dodecyl sulfate-polyacrylamide gel electrophoresis (SDS-PAGE) on a SuperSep Ace gel (Wako), as described by Laemmli [17]. After electrophoresis, the gel was observed under a fluorescent imager to confirm the probe labeling of the protein, followed by staining with a Quick-CBB staining kit (Wako). Precision Plus Protein Dual Color Standards (Bio-Rad) were used as the protein standards.

ELISA

The antigen-binding activity of the Fab fragments and UQ-bodies were tested using ELISA. A 96-well microplate (Greiner bio-one, Tokyo, Japan) was coated overnight with 100 µl per well of streptavidin (10 µg/ml) in phosphate-buffered saline (PBS) at 16 °C. Some of the wells were washed and added with bio-DAE10 and incubated for 30 min. The plate was then blocked at 25 °C for 2 h with 20% ImmunoBlock (DS Pharma Biomedical Co., Ltd.), washed three times with PBST (0.2% Tween 20 in PBS), and incubated with 100 µl/well of PBS containing 5 µg/ml of Fab or UQ-bodies at 25 °C for 1 h. The plate was washed three times again with PBST, and incubated with 100 µl/well of 5000-fold diluted HRP/anti-His monoclonal conjugate (Wako) in PBS at 25 °C for 1 h. The plate was then washed three times with PBST again and developed with 100 µl/well TMBZ solution [100 µg/ml 3,3′,5,5′-tetramethylbenzidine (Sigma) and 0.04 µl/ml H_2O_2, in 100 mM NaOAc, pH 6.0]. After incubation for 5–30 min, the reaction was stopped by adding 50 µl/well of 10%

sulfuric acid, and the absorbance was read using a Model 680 microplate reader (Bio-Rad, Tokyo, Japan) at 450 nm, with 655 nm as the control.

Evaluation of the affinity of UQ-bodies

The affinity of UQ-bodies against biotinylated DAE10 was investigated using a biolayer interferometry (BLI)-based biosensor BLItz system (FortéBio, Pall, Menlo Park, CA, USA). BLI is a label-free technology to measure biomolecular interactions within the interactome [18]. For immobilization onto the biosensor chips, biotinlylated DAE10 was diluted to 100 nM in kinetics buffer (10 mM sodium phosphate, 150 mM NaCl, 0.002% Tween 20, 0.1% bovine serum albumin, pH 7.4) and added to a streptavidin biosensor chip (Pall FortéBio, Fremont, CA). The UQ-body concentration was adjusted to 100, 200, 400, and 800 nM, and 4 μl each in kinetics buffer (Pall FortéBio) were used as analytes. After immobilization of biotinylated DAE10, a baseline was taken by running the sensor chip in kinetics buffer for 60 s, followed by the addition of the UQ-bodies to obtain the association curve for 120 s. By soaking in 250 μl of kinetics buffer for 120 s, the dissociation curve was obtained. The sensor chip was then regenerated by soaking in 100 mM glycine solution (pH 3) for 120 s. The association rate (k_{on}) and dissociation rate (k_{off}) constants, as well as their standard errors, were calculated by fitting the curves using the BLItz software. The K_A value was calculated by dividing k_{on} by k_{off}. The standard error (SE) of the ratio was calculated according to

$$\frac{M_1 \pm \varepsilon_1}{M_2 \pm \varepsilon_2} = \frac{M_1}{M_2} \pm \sqrt{\left(\frac{1}{M_2} \cdot \varepsilon_1\right)^2 + \left(\frac{M_1}{{M_2}^2} \cdot \varepsilon_2\right)^2} \qquad (1)$$

where M_1 (M_2) and ε_1 (ε_2) are the mean and SE of k_{on} (k_{off}), respectively.

Fluorescence measurement

Purified UQ-bodies (25 ng) in 250 μl of PBST containing 1% BSA were added into a 5 mm × 5 mm quartz cell (Jasco, Tokyo, Japan), and 2.5 μl of untreated Aβ42 or ADDL at variable concentrations was added by titration. After each addition, the solution was incubated at 25 °C for 5 minutes before the spectral measurements. As a control, quartz cells containing the same volume and amount of UQ-bodies were added with PBS instead of the analyte solution. The fluorescence spectra were obtained at 25 °C using a fluorescence spectrophotometer Model FP-8500 (Jasco) with excitation at 520 nm or 546 nm, for ATTO520 and TAMRA, respectively. The excitation and emission slit widths were set to 5.0 nm. Dose-response curves were fitted to a 4-parameter logistic equation at the maximum emission wavelength, using Kaleida Graph 4.1 (Synergy Software, Reading, PA, USA) and the EC_{50} value (the concentration of an antigen that gives a half-maximal response) with its SE was calculated from the curve. The limit of detection (LOD) was obtained as the estimated antigen concentration that shows the mean blank value plus three standard deviations (SDs).

Imaging of Aβ oligomers

To image Aβ oligomers, 200 μl overnight-incubated Aβ42 peptide at a higher concentration of 250 μM was added with 100 ng of double ATTO520-labeled UQ-bodies and incubated for 30 min at room temperature on a rotating wheel. The samples were then imaged using a fluorescence microscope IX71 (Olympus, Tokyo, Japan) equipped with 470 ± 20 nm excitation and 520 ± 20 nm emission filters. The images were obtained using the HC Image system equipped with an ImagEM EM-CCD camera (Hamamatsu Photonics, Japan).

Results

Design of the UQ-bodies

A UQ-body is an antibody fragment site-specifically labeled with a fluorescent dye(s) at a position(s) that enables antigen-dependent fluorescence emission. In this study, we designed three formats of Fab fragment to prepare UQ-bodies. One was a single-label format at the N-terminus of V_H-C_H1 (Fd fragment), as shown in Figure 1A. To investigate the influence of the distance between the V_H N-terminus and the dye, we also inserted a GS linker between the C-terminus of the Cys-tag and the N-terminus of V_H (Figure 1B). The third vector was designed to enable double-labeling, i.e. two Cys-tags with a GS linker at both Fd and light chains were appended, as shown in Figure 1C.

Preparation of UQ-bodies

Fab fragments expressed in *E. coli* were purified using an immobilized metal affinity gel, and then labeled with TMRC5, TMRC6, or ATTO520-maleimide. Labeled antibody fragments were further purified using anti-DYKDDDDK antibody-coated beads. All the prepared UQ-bodies were separated by SDS-PAGE and the fluorescence of Fab fragments was observed under a fluorescence transilluminator. Figure 2A shows the CBB-stained and unstained fluorescence of SDS-PAGE for the ATTO520-labeled UQ-bodies. All three UQ-bodies, 1Hh12A11-ATTO520 (lane 1), 1HGSh12A11-ATTO520 (lane 2), and 2GSh12A11-ATTO520 (lane 3) were purified, and fluorescence of the expected bands was observed, suggesting that all the proteins were successfully labeled with ATTO520-maleimide. Only one main band was observed on the CBB-stained gel for 1Hh12A11-ATTO520 and 1HGSh12A11-ATTO520. Since another band with lower mobility (labeled L chain) was observed in lane 3, the main band in these lanes represents the

co-migrating (labeled Fd)-L chains. It is worth noting that faster migrating minor fluorescent bands are also observed for each lane. Probably, these bands represent partially degraded Fd chain at its C-terminal region, which might be also labeled at the internal Cys residues in C_H1 domain, due to imperfect folding in *E. coli* cytoplasm. Next, the antigen-binding activity of the UQ-bodies was confirmed using ELISA. Figure 2B shows the binding activity of the prepared UQ-bodies. All three kinds of UQ-bodies bound to the immobilized DAE10 peptide (an antigen peptide containing $A\beta_{1-7}$ epitope), but not to streptavidin.

The antigen binding affinity of the UQ-bodies was evaluated using BLItz. The K_D values of 1Hh12A11-ATTO520, 1HGSh12A11-ATTO, and 2GSh12A11-ATTO520 against immobilized bio-DAE10 were 61.3 ± 3.5 μM, 6.08 ± 0.36 μM, and 275 ± 21.5 nM, respectively.

The SDS-PAGE images of CBB-stained and fluorescence of UQ-bodies prepared with TMRC5 and TMRC6 are shown in Figure S1A and Figure S2A, respectively. Although the bands with the expected molecular weights were labeled successfully, the faster migrating bands were also observed with higher intensities than ATTO520-labeled UQ-bodies. All the UQ-bodies showed antigen-binding activity, as shown in Figure S1B and Figure S2B. Compared with single TAMRA-labeled UQ-bodies, lower binding activity was observed for double TAMRA-labeled UQ-bodies.

De-quenching of UQ-bodies with denaturants or antigen

In UQ-bodies, fluorescent dyes might be quenched by the Trp residues in the variable regions, or the other dye in the double-labeled UQ-body. Therefore, the purified UQ-bodies were treated with 7 M guanidine hydrochloride solution with 100 mM dithiothreitol (DTT) to evaluate the degree of quenching, which is a good parameter to evaluate its potential as a

UQ-body. As shown in Figure 3A–C and Table 2, the fluorescence intensities of 1Hh12A11-ATTO520, 1HGSh12A11-ATTO520, and 2GSh12A11-ATTO520 increased by 1.32-, 1.30- and 6.94-fold, respectively. Although the degrees of de-quenching for the two single-labeled UQ-bodies were similar, the double-labeled UQ-body showed superior de-quenching, suggesting its potential as a good UQ-body. Similar results were observed for the TAMRA-labeled UQ-bodies. As shown in Table 2, the de-quenching of double-labeled UQ-bodies was much higher than that of the single labeled UQ-bodies.

When the antigen dependency of fluorescent response was evaluated using a fluorescence spectrometer, a significant antigen (bio-DAE10)-dependent fluorescence increase was observed for the ATTO520 double-labeled UQ-bodies (Figure 3 D–F) and TAMRA double-labeled UQ-bodies (Table 2). However, single-labeled UQ-bodies were not significantly de-quenched by the addition of the antigen.

Bio-DAE10 dose-response curve with double-labeled UQ-bodies

Double-labeled UQ-bodies were used to evaluate their antigen dose response. Figure S1C and Figure S2C show the fluorescent spectra for 2GSh12A11-TMRC5 and -TMRC6, respectively. With increasing antigen (bio-DAE10) concentration, a significant increase in fluorescence intensity was observed. Based on these data, dose-response curves to detect the antigen with both UQ-bodies were constructed (Figure S1D and S2D). Similar results for 2GSh12A11-ATTO520 were also obtained (not shown).

Detection of Aβ peptide and ADDL

UQ-body 2GSh12A11-ATTO520 was used to detect untreated Aβ42 peptide and ADDL. As show in Figure 4A and Figure 4B, with the increasing concentration of amyloid-β peptide

and ADDL, the fluorescence intensities of the UQ-bodies increased by 2.2-fold and 2.8-fold, respectively. Does-response curves to detect the Aβ42 peptide and ADDL were obtained (Figure 4C). We also calculated the EC_{50} and LOD of UQ-body assay to compare the responses of the UQ-bodies for the peptides and oligomers. By curve fitting, an EC_{50} value of $1.09 \pm 0.04 \times 10^{-6}$ M for ADDL was obtained, which was smaller than that for the untreated Aβ42 peptide ($33 \pm 26 \times 10^{-6}$ M). The LODs for the two antigens were calculated as 2.0×10^{-7} M and 3.0×10^{-7} M, respectively. These results indicated that both the Aβ42 peptide and ADDL were successfully detected by the UQ-bodies, with higher sensitivity to ADDL.

Bio-imaging of Aβ oligomers

To show the UQ-body's potential as a bioimaging reagent, Aβ oligomers were imaged under a fluorescence microscope using ATTO520 double-labeled UQ-bodies. As shown in Figure 5, the UQ-bodies clearly showed the fluorescence in the presence of Aβ oligomer, while those without Aβ oligomers did not.

Discussions and Conclusions

In this study, we prepared three formats of Fab: Single-labeled Fab without a GS linker, single-labeled Fab with a GS linker, and a double-labeled Fab with a GS linker on both chains of Fab. Although the antigen-dependent fluorescence was not significant for the single-labeled UQ-bodies, the overall length of the linker between the dye and the N-terminus of antibody V_H is still considered important. As shown in Table 2, the UQ-bodies with a GS linker between the Cys-tag and the antibody V_H showed higher de-quenching when they were chemically denatured, especially for the TAMRA-labeled UQ-bodies. In

addition, the TAMRA-C6 labeled UQ-bodies showed greater de-quenching than the TAMRA-C5 labeled ones. The longer linker might have allowed the dye to move closer to the Trp residues in the variable region, which would increase the quenching of the UQ-body in the native state without the antigen.

For all three fluorescent dyes used, the double-labeled UQ-bodies showed higher antigen responses. A plausible mechanism for the higher quenching observed for the double-labeled UQ-bodies is the dye-dye quenching due to H-dimer formation [19] between the two dyes introduced into the Fd and L chains. More specifically, the double ATTO520-labeled UQ-body showed higher response than the double TAMRA-labeled UQ-bodies. Compared with TAMRA-C5 labeled UQ-body, ATTO520-labeled UQ-body has a lower tendency to form stable H-dimers [3]. Although H-dimer formation is important for the efficient quenching of double-labeled UQ-bodies, if the formed dimer is too stable, it can affect the UQ-body's sensitivity and response, because the dye-dye interaction competes with antigen binding. Probably, the stronger H-dimer formed using TAMRA was more inhibitory to antigen binding as observed in ELISA signals (Figures S1B and S2B), suggesting ATTO520 as a more suitable label.

By contrast, the quenching of a single dye incorporated into an UQ-body is considered to occur solely by the Trp residues in its variable region through a photoinduced electron transfer mechanism [1, 20-22]. According to the amino acid sequences, in the variable region of h12A11, there are five Trp residues in Fd and one in the L chain. Some of these Trp residues directly or indirectly interact with the fluorescent dye, and provide electrons to the excited dye, resulting in the molecule returning to its ground state without emitting fluorescence.

Currently, bioimaging of live cells is a challenging task for biotechnologists and analytical

chemists, because at least one washing step is necessary to remove the background fluorescence signal. In this study, we demonstrated that UQ-bodies could be used to stain Aβ samples without any wash steps. Given that aggregation of Aβ is formed mainly on the cell surface, it might also be possible that UQ-body could detect the target localized on the cellular membrane *in vivo*. On the other hand, since the concentration of the Aβ in body fluid is relatively low (pM ~ sub nM range [23]), enrichment of such samples would enable effective detection. Taken together, the results suggested the utility of the UQ-bodies as useful tools to study the process of Aβ oligomerization and its application in AD diagnosis.

Acknowledgments

We thank the Dynamic Alliance for Open Innovation Bridging Human, Environment, and Materials from MEXT, Japan, for support. We also thank the Division of Biomaterial Analysis, Technical Department, Tokyo Institute of Technology for the nucleic acid sequence analysis.

Funding source

This work was supported partly by a Developing Research Grant from the Nakatani Foundation, Japan; by JSPS KAKENHI (Grant Numbers JP15H04191 and JP26420793) from the Japan Society for the Promotion of Science, Japan; by the National Natural Science Foundation of China (Grant Number: 21775064) and Shandong Provincial Natural Science Foundation (Grant Number: ZR2017MB037).

References

[1] R. Abe, H. Ohashi, I. Iijima, M. Ihara, H. Takagi, T. Hohsaka, H. Ueda, "Quenchbodies": quench-based antibody probes that show antigen-dependent fluorescence, J Am Chem Soc, 133 (2011) 17386-17394.

[2] H. Ueda, J. Dong, From fluorescence polarization to Quenchbody: Recent progress in fluorescent reagentless biosensors based on antibody and other binding proteins, Biochim Biophys Acta, 1844 (2014) 1951-1959.

[3] R. Abe, H.J. Jeong, D. Arakawa, J. Dong, H. Ohashi, R. Kaigome, F. Saiki, K. Yamane, H. Takagi, H. Ueda, Ultra Q-bodies: quench-based antibody probes that utilize dye-dye interactions with enhanced antigen-dependent fluorescence, Sci Rep, 4 (2014) 4640.

[4] S. Zhao, J. Dong, H.-J. Jeong, K. Okumura, H. Ueda, Rapid detection of the neonicotinoid insecticide imidacloprid using a quenchbody assay, Anal. Bioanal. Chem., (2018). doi:10.1007/s00216-018-1074-y

[5] H.J. Jeong, T. Kawamura, M. Iida, Y. Kawahigashi, M. Takigawa, Y. Ohmuro-Matsuyama, C.I. Chung, J. Dong, M. Kondoh, H. Ueda, Development of a Quenchbody for the Detection and Imaging of the Cancer-Related Tight-Junction-Associated Membrane Protein Claudin, Anal Chem, 89 (2017) 10783-10789.

[6] D.L. Price, New perspectives on Alzheimer's disease, Annu Rev Neurosci, 9 (1986) 489-512.

[7] K. Blennow, M.J. de Leon, H. Zetterberg, Alzheimer's disease, Lancet, 368 (2006) 387-403.

[8] C. Geula, Abnormalities of neural circuitry in Alzheimer's disease: hippocampus and cortical cholinergic innervation, Neurology, 51 (1998) S18-29; discussion S65-17.

[9] E.A. Grace, J. Busciglio, Aberrant activation of focal adhesion proteins mediates fibrillar

amyloid beta-induced neuronal dystrophy, J Neurosci, 23 (2003) 493-502.

[10] J. Busciglio, A. Lorenzo, J. Yeh, B.A. Yankner, beta-amyloid fibrils induce tau phosphorylation and loss of microtubule binding, Neuron, 14 (1995) 879-888.

[11] H.J. Kim, K.W. Park, T.E. Kim, J.Y. Im, H.S. Shin, S. Kim, D.H. Lee, B.S. Ye, J.H. Kim, E.J. Kim, K.H. Park, H.J. Han, J.H. Jeong, S.H. Choi, S.A. Park, Elevation of the Plasma Abeta40/Abeta42 Ratio as a Diagnostic Marker of Sporadic Early-Onset Alzheimer's Disease, J Alzheimers Dis, 48 (2015) 1043-1050.

[12] J.A. Kim, M. Kim, S.M. Kang, K.T. Lim, T.S. Kim, J.Y. Kang, Magnetic bead droplet immunoassay of oligomer amyloid beta for the diagnosis of Alzheimer's disease using micro-pillars to enhance the stability of the oil-water interface, Biosens Bioelectron, 67 (2015) 724-732.

[13] M. Sakono, T. Zako, Amyloid oligomers: formation and toxicity of Abeta oligomers, The FEBS journal, 277 (2010) 1348-1358.

[14] T. Zako, Amyloid oligomers, The FEBS journal, 277 (2010) 1347.

[15] M.P. Lambert, A.K. Barlow, B.A. Chromy, C. Edwards, R. Freed, M. Liosatos, T.E. Morgan, I. Rozovsky, B. Trommer, K.L. Viola, P. Wals, C. Zhang, C.E. Finch, G.A. Krafft, W.L. Klein, Diffusible, nonfibrillar ligands derived from Abeta1-42 are potent central nervous system neurotoxins, Proc Natl Acad Sci U S A, 95 (1998) 6448-6453.

[16] G.S. Basi, H. Feinberg, F. Oshidari, J. Anderson, R. Barbour, J. Baker, T.A. Comery, L. Diep, D. Gill, K. Johnson-Wood, A. Goel, K. Grantcharova, M. Lee, J. Li, A. Partridge, I. Griswold-Prenner, N. Piot, D. Walker, A. Widom, M.N. Pangalos, P. Seubert, J.S. Jacobsen, D. Schenk, W.I. Weis, Structural correlates of antibodies associated with acute reversal of amyloid beta-related behavioral deficits in a mouse model of Alzheimer disease, J Biol Chem, 285 (2010) 3417-3427.

[17] U.K. Laemmli, Cleavage of structural proteins during the assembly of the head of bacteriophage T4, Nature, 227 (1970) 680-685.

[18] R.L. Rich, D.G. Myszka, Higher-throughput, label-free, real-time molecular interaction analysis, Anal Biochem, 361 (2007) 1-6.

[19] M. Ogawa, N. Kosaka, P.L. Choyke, H. Kobayashi, H-type dimer formation of fluorophores: a mechanism for activatable, in vivo optical molecular imaging, ACS Chem Biol, 4 (2009) 535-546.

[20] V. Buschmann, K.D. Weston, M. Sauer, Spectroscopic study and evaluation of red-absorbing fluorescent dyes, Bioconjug Chem, 14 (2003) 195-204.

[21] N. Marme, J.P. Knemeyer, M. Sauer, J. Wolfrum, Inter- and intramolecular fluorescence quenching of organic dyes by tryptophan, Bioconjug Chem, 14 (2003) 1133-1139.

[22] A.C. Vaiana, H. Neuweiler, A. Schulz, J. Wolfrum, M. Sauer, J.C. Smith, Fluorescence quenching of dyes by tryptophan: interactions at atomic detail from combination of experiment and computer simulation, J Am Chem Soc, 125 (2003) 14564-14572.

[23] J. Waters, The Concentration of Soluble Extracellular Amyloid-β Protein in Acute Brain Slices from CRND8 Mice, PLOS ONE, 5 (2011) e15709.

Table 1. Oligonucleotides used in this study.

Primer name	Sequences (5'-3')
Age_VHh12A11	GCTCTAATGAGACCGGTCAGGTTCAGCTGGTTGAATC
JHXho_h12A11	GGAAGCGCTCGAGACTGTCACTGTAGTGCCTTGAC
RV_Vkh12A11	AAGGAGATATCACATGTCTACAGACGTTGTCATGACCCA
JkHind_h12A11	GGGTTTCAAGCTTGGCCGCTTTAATCTCCAGTTTA
Spe_Vkh12A11	TCTAATGAGACTAGTTCTACAGACGTTGTCATGACC
T7promoter	TAATACGACTCACTATAGGG
T7terminator	TAGTTATTGCTCAGCGGTGG

Table 2. Dequenching of UQ-bodies with 7 M GdnHCl/100 mM DTT or 28.8 μM antigen.*

Quenchbody name	Dye	GdnHCl/DTT	bio-DAE10
1Hh12A11-ATTO520	ATTO520	1.32	1.0
1HGSh12A11-ATTO520	ATTO520	1.30	1.0
2h12A11-ATTO520	ATTO520	6.24	1.79
1Hh12A11-TMRC5	TAMRA-C5	1.20	1.0
1HGSh12A11-TMRC5	TAMRA-C5	1.35	1.1
2h12A11-TMRC5	TAMRA-C5	5.12	2.1
1Hh12A11-TMRC6	TAMRA-C6	1.29	1.0
1HGSh12A11-TMRC6	TAMRA-C6	1.6	1.07
2h12A11-TMRC6	TAMRA-C6	5.05	1.81

* Numbers denote fold increase in fluorescence

Figure legends

Figure 1. Constructs for preparation of UQ-bodies. Cys-tag: MAQIEVNCSNET for Fd and MSKQCSNETS for L chain; GS linker: GGGSGGTG for Fd and GGGSGGTS for L chain.

Figure 2: SDS-PAGE, fluorescence analysis (**A**) and antigen binding activity (**B**) of prepared UQ-bodies with ATTO520-maleimide. M: Protein marker; Lane 1: 1Hh12A11A-ATTO520; lane 2: 1HGSh12A11-ATTO520; lane 3: 2GSh12A11-ATTO520.

Figure 3. Fluorescence spectra comparison under denaturing condition (**A, B, C**) and by the addition of antigen (**D, E, F**). A, D: 1Hh12A11-ATTO520; B, E: 1HGSh12A11-ATTO520; C, F: 2GSh12A11-ATTO520.

Figure 4. Fluorescence spectral change upon addition of untreated Aβ42 (**A**), ADDL (**B**), and dose-response curves (**C**) for Aβ42 and ADDL with 2GSh12A11-ATTO520.

Figure 5. Fluorescence imaging of Aβ oligomers by ATTO520-labeled 2GS UQ-body.

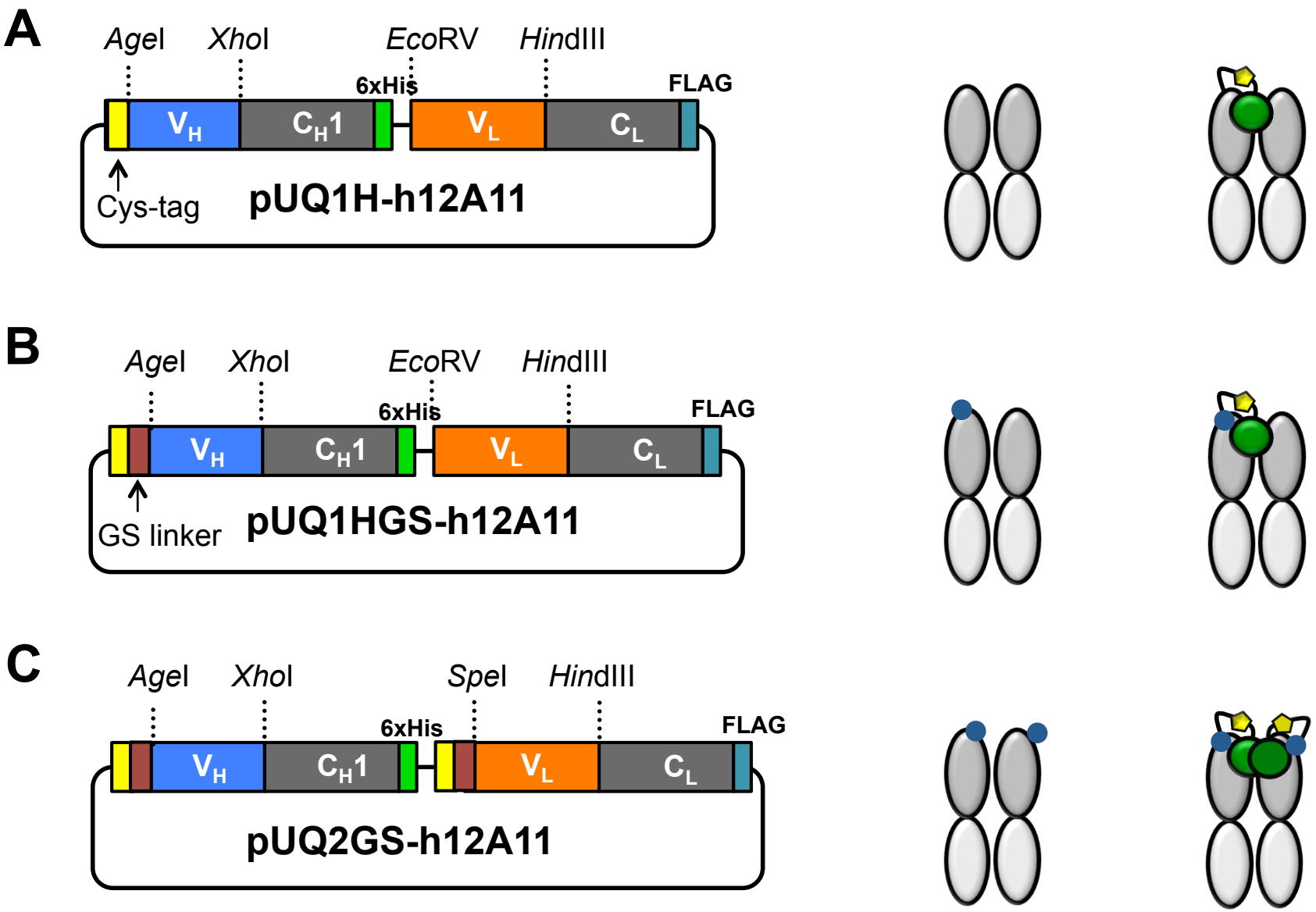

Fig. 1

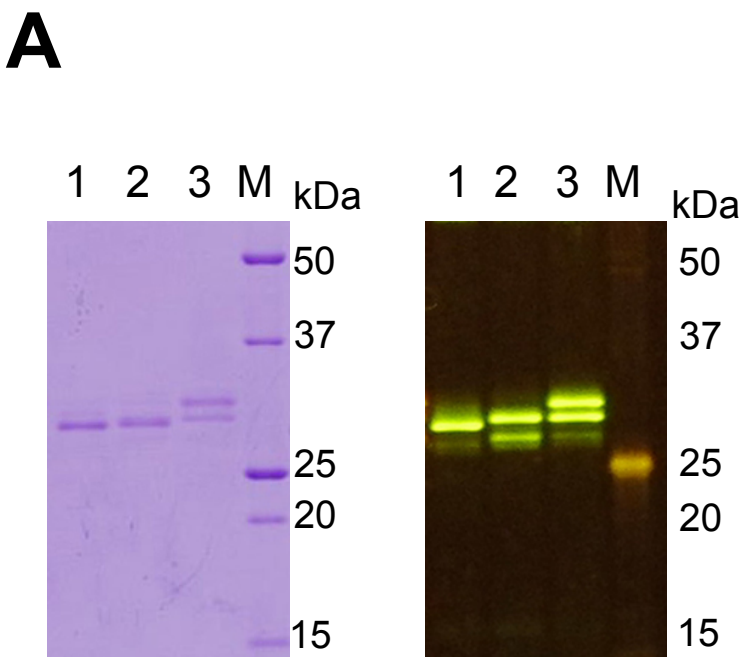

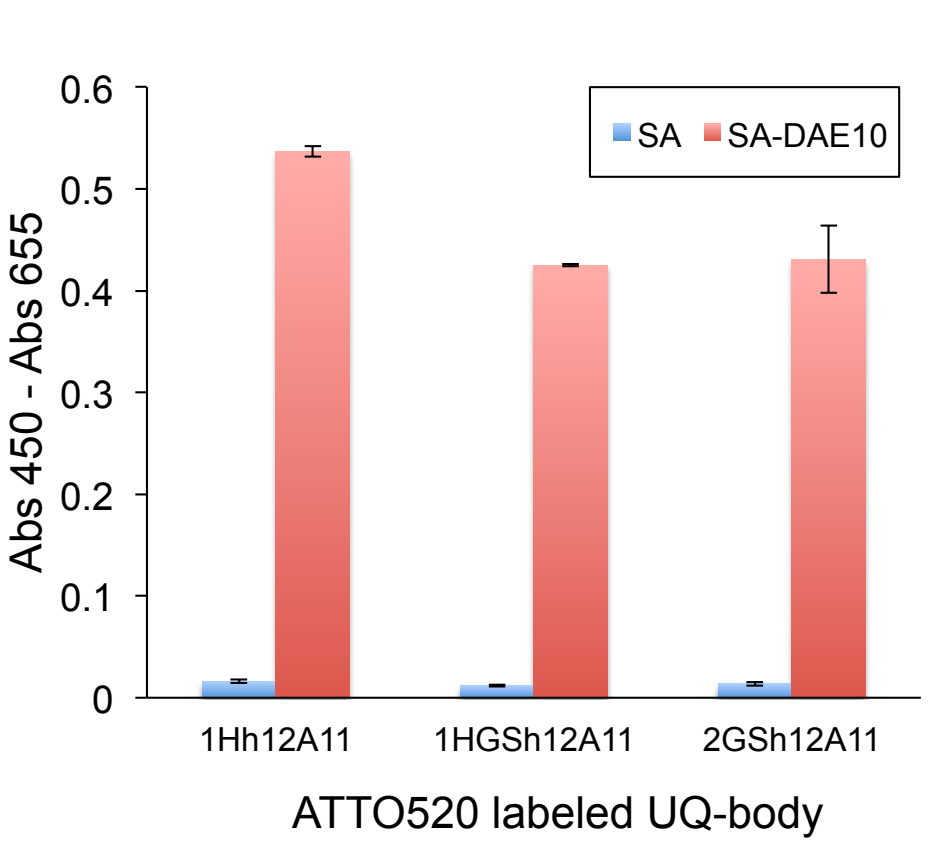

Fig. 2

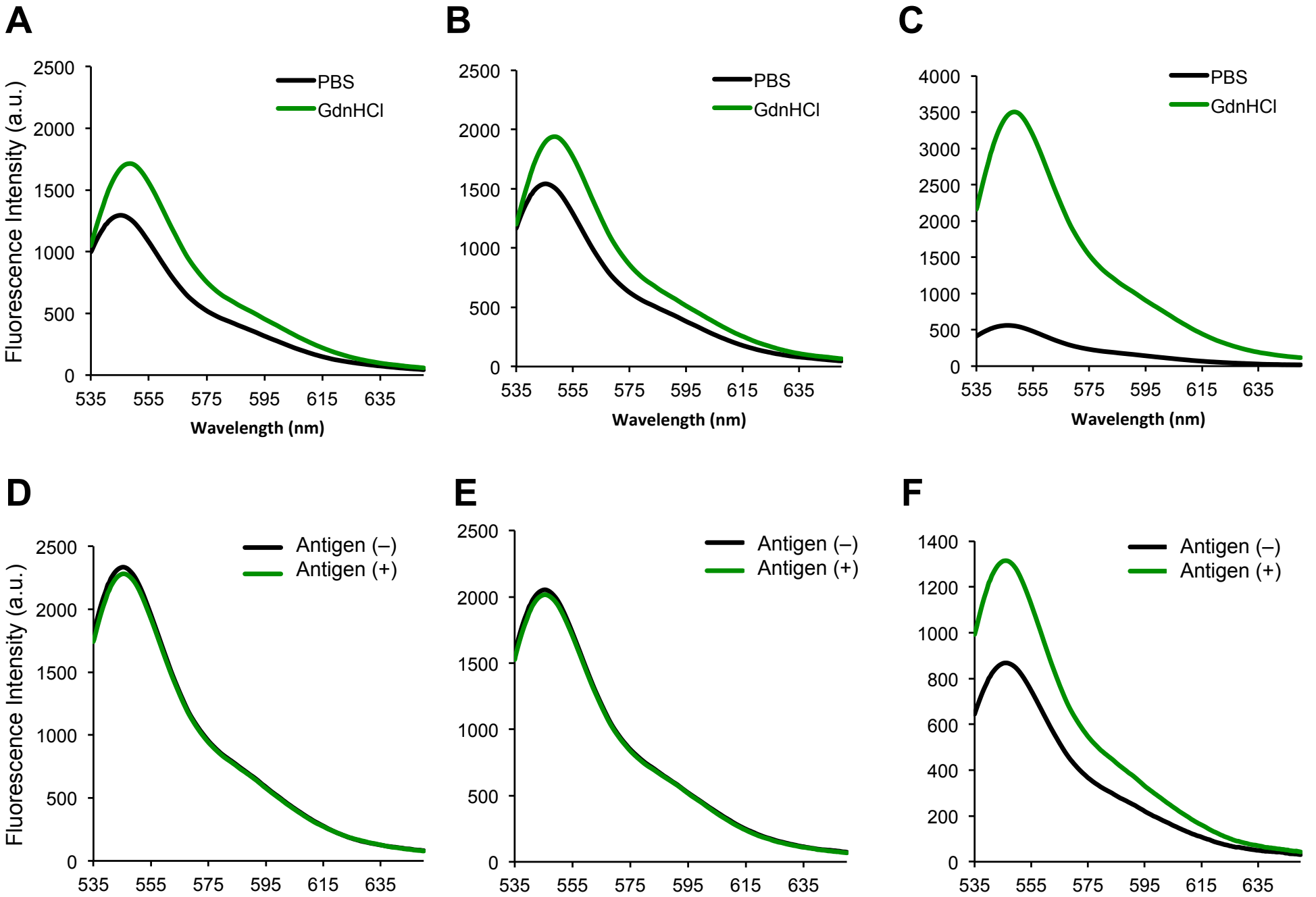

Fig. 3

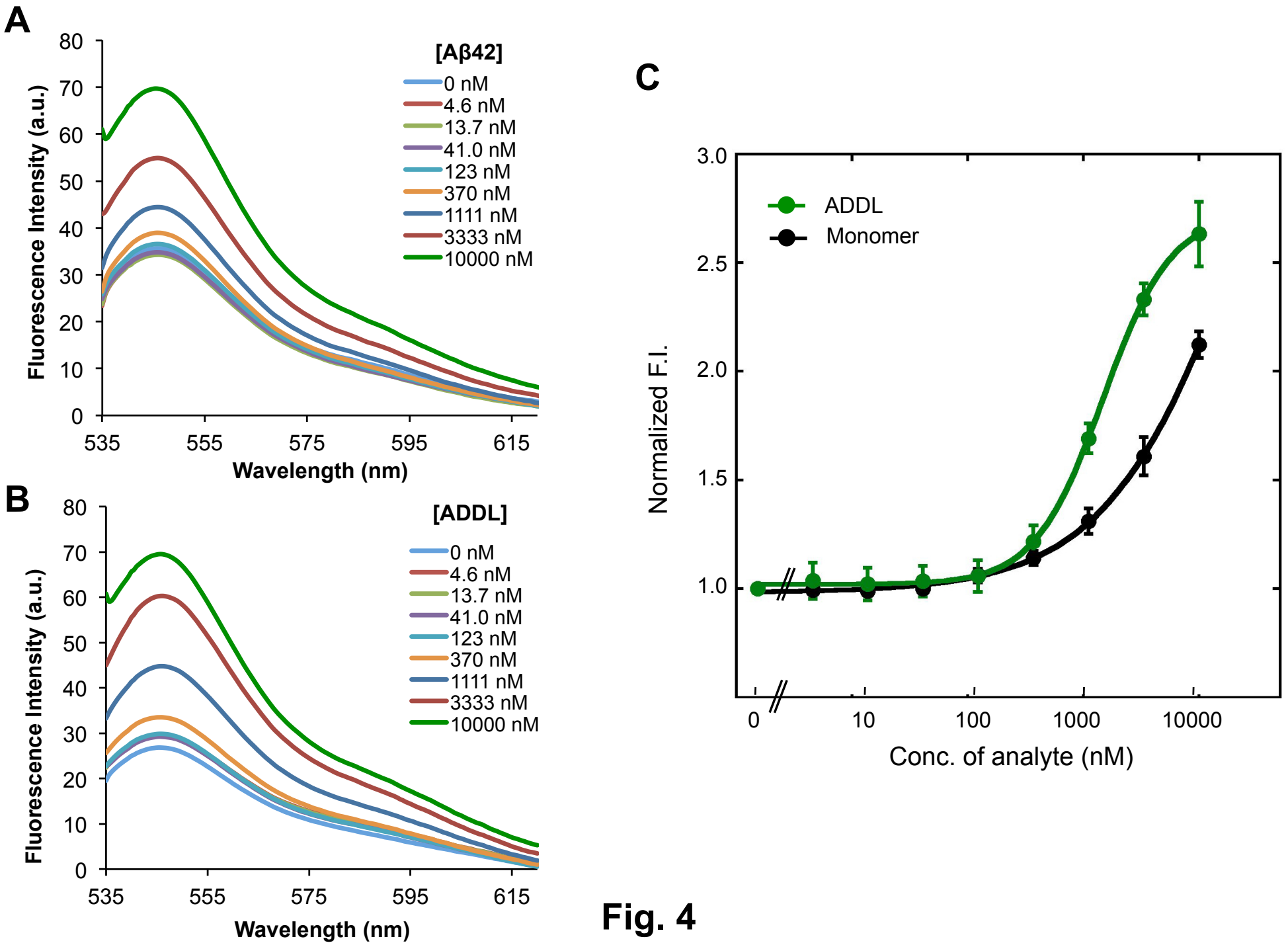

Fig. 4

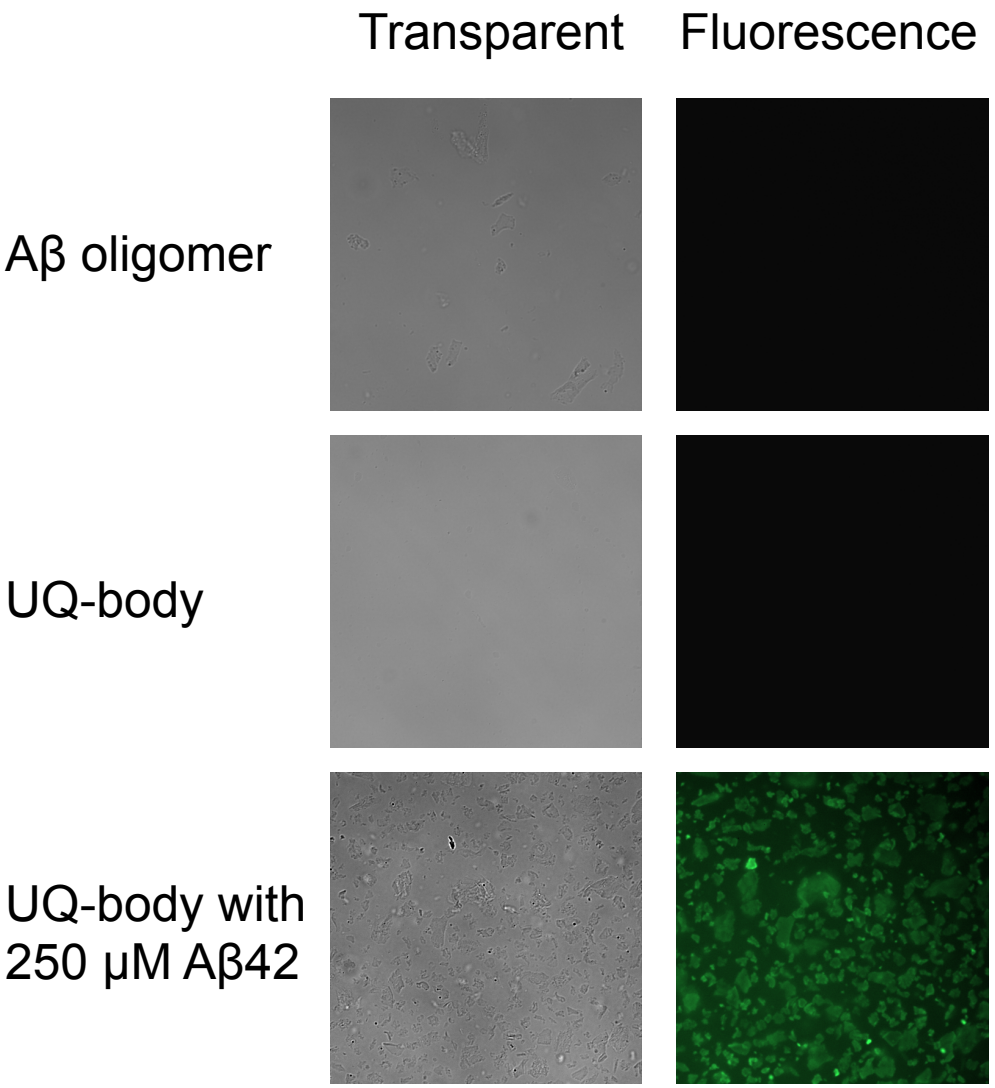

Fig. 5